



## Characteristics of Complex Fractionated Atrial Electrogram in the Electroanatomically Remodeled Left Atrium of Patients With Atrial Fibrillation

Jae Hyung Park, BSc; Sang Weon Park, MD, PhD; Jong Youn Kim, MD; Sook Kyoung Kim; Boyoung Jeoung, MD, PhD; Moon-Hyung Lee, MD, PhD; Chun Hwang, MD; Young-Hoon Kim, MD, PhD; Sung Soon Kim, MD, PhD; Hui-Nam Pak, MD, PhD

**Background:** Complex fractionated atrial electrogram (CFAE) guided ablation is effective in some patients with persistent atrial fibrillation (PeAF), but the pattern of CFAE may be different in the remodeled left atrium (LA).

**Methods and Results:** In 100 AF patients (83 males, 55.0±10.6 years old) with AF (51 paroxysmal AF (PAF), 49 PeAF) who underwent catheter ablation, CFAE cycle length (CL) and distribution (NavX 3D map) were compared according to the LA volume (3D-CT) and endocardial voltage (during high right atrial pacing 500-ms (Vol<sub>PACE</sub>) and AF (Vol<sub>AF</sub>; NavX). The mean CFAE-CL was longer (P=0.003) and the % area CFAE was smaller (P=0.006) in patients with LA ≥125 ml than those with <125 ml. The mean CFAE-CL was longer in patients with Vol<sub>PACE</sub> <1.7 mV than those with ≥1.7 mV (P=0.002) and in Vol<sub>AF</sub> <0.7 mV than ≥0.7 mV (P<0.001). The % area CFAE was smaller in patients with Vol<sub>PACE</sub> <1.7 mV than those with ≥1.7 mV (P=0.006). The incidence of septal CFAE was consistently high, regardless of the degree of LA remodeling.

**Conclusions:** In the AF patients with an electroanatomically remodeled LA, the % area of CFAE was smaller and mean CFAE-CL was longer than in those with a less remodeled LA. However, the majority of CFAE are consistently positioned on the septum in the remodeled LA. (*Circ J* 2010; **74**: 1557–1563)

**Key Words:** Atrial fibrillation; Computed tomography; Left atrium; Morphological remodeling; Voltage mapping

Although radiofrequency catheter ablation (RFCA) of atrial fibrillation (AF) is an effective treatment modality for controlling AF,<sup>1</sup> circumferential pulmonary vein (PV) ablation is not enough in some patients, especially those with persistent AF (PeAF).<sup>2,3</sup> Nademanee et al reported that complex fractionated atrial electrogram (CFAE)-guided left atrial (LA) ablation terminated sustained AF in 95% of patients, resulting in excellent clinical outcomes (1 year AF-free rate, 91% with combined ibutilide medication in 28% of patients).<sup>4</sup> They also reported that maintenance of sinus rhythm (SR) after CFAE-guided LA ablation improved mortality rates.<sup>5</sup> However, clinical outcomes of CFAE-guided ablation studies have been quite variable,<sup>6–10</sup> and the electrophysiologic mechanism of CFAE has not yet been clearly elucidated. We previously characterized CFAE as being predominantly located at the septum, roof, and LA appendage (LAA), with low voltage surrounded by a high voltage area and low conduction velocity in patients with AF.<sup>11</sup> We also demonstrated electroanatomical remodeling of the LA in patients with PeAF, compared with

paroxysmal AF (PAF), by analyzing LA volume and LA voltage.<sup>12,13</sup> However, CFAE in patients with an electroanatomically remodeled LA has not been clearly characterized yet. Therefore, we hypothesized that the CFAE pattern (ie, CFAE-cycle length (CL) or distribution) will be different in patients with a remodeled atrium. In the present study we compared the CFAE-CL and % area of CFAE in patients with an enlarged LA and those without LA enlargement by analyzing 3D-computed tomographic (CT) images and NavX voltage mapping. We also compared the distribution of CFAE in patients with low and high LA voltages.

### Methods

#### Patient Selection

The study protocol was approved by the Institutional Review Board and all patients provided written informed consent. We enrolled 100 patients with AF (M/F=83/17, mean age 55.0±10.6 years) who underwent RFCA. Among them, 51 patients had PAF, and 49 had PeAF. The exclusion criteria

Received January 25, 2010; accepted April 1, 2010; released online June 16, 2010 Time for primary review: 49 days  
Yonsei University Health System, Seoul (J.H.P., J.Y.K., S.K.K., B.J., M.-H.L., S.S.K., H.-N.P.); Korea University College of Medicine, Seoul (S.W.P., Y.-H.K.), Republic of Korea; and Krannert Heart Institute, Indianapolis University, Indianapolis, IN (C.H.), USA  
Mailing address: Hui-Nam Pak, MD, PhD, Yonsei University Health System, 250 Seongsanno, Seodaemun-gu, Seoul 120-752, Republic of Korea. E-mail: hnpak@yuhs.ac

ISSN-1346-9843 doi:10.1253/circj.CJ-10-0048

All rights are reserved to the Japanese Circulation Society. For permissions, please e-mail: [cj@j-circ.or.jp](mailto:cj@j-circ.or.jp)

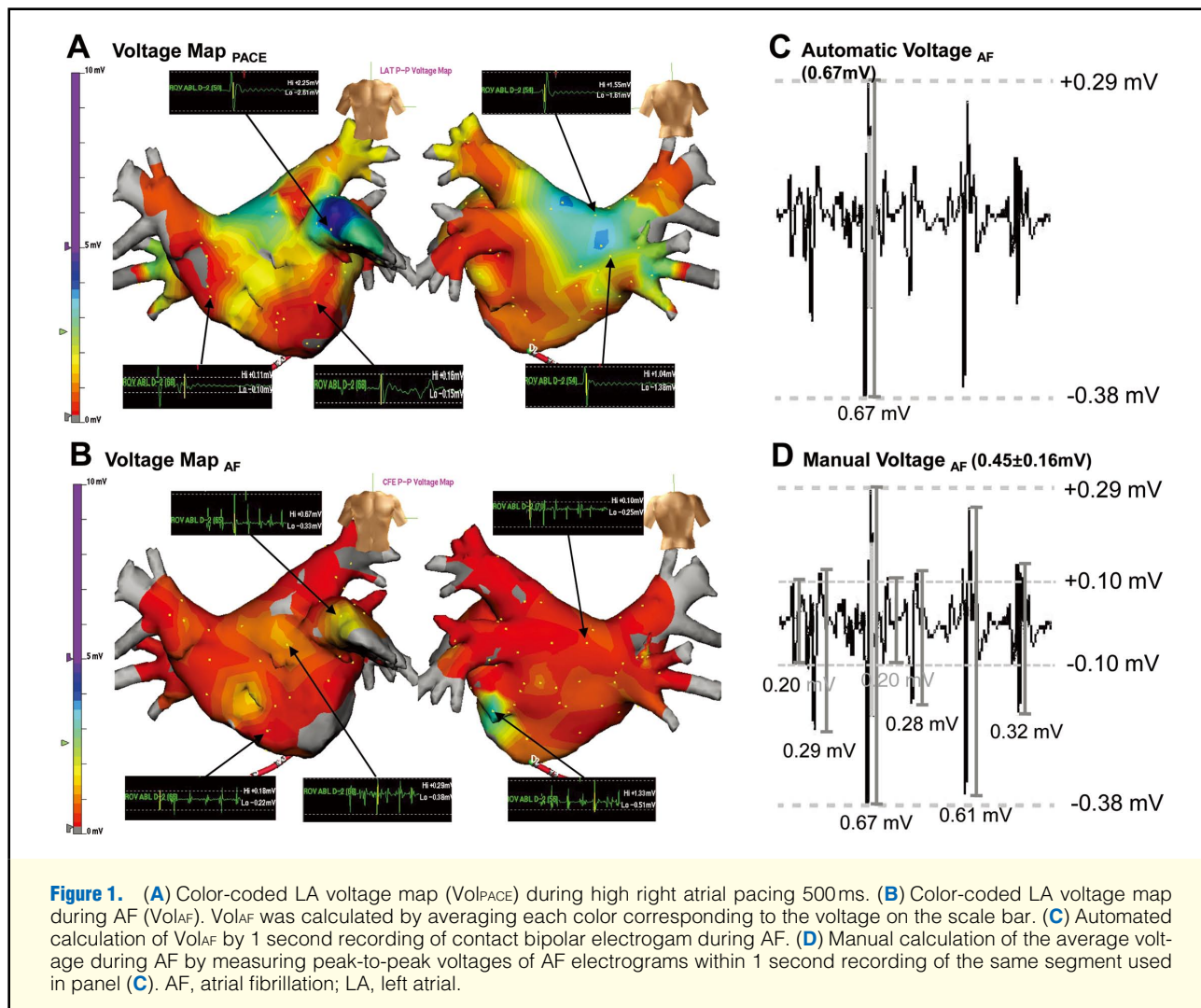


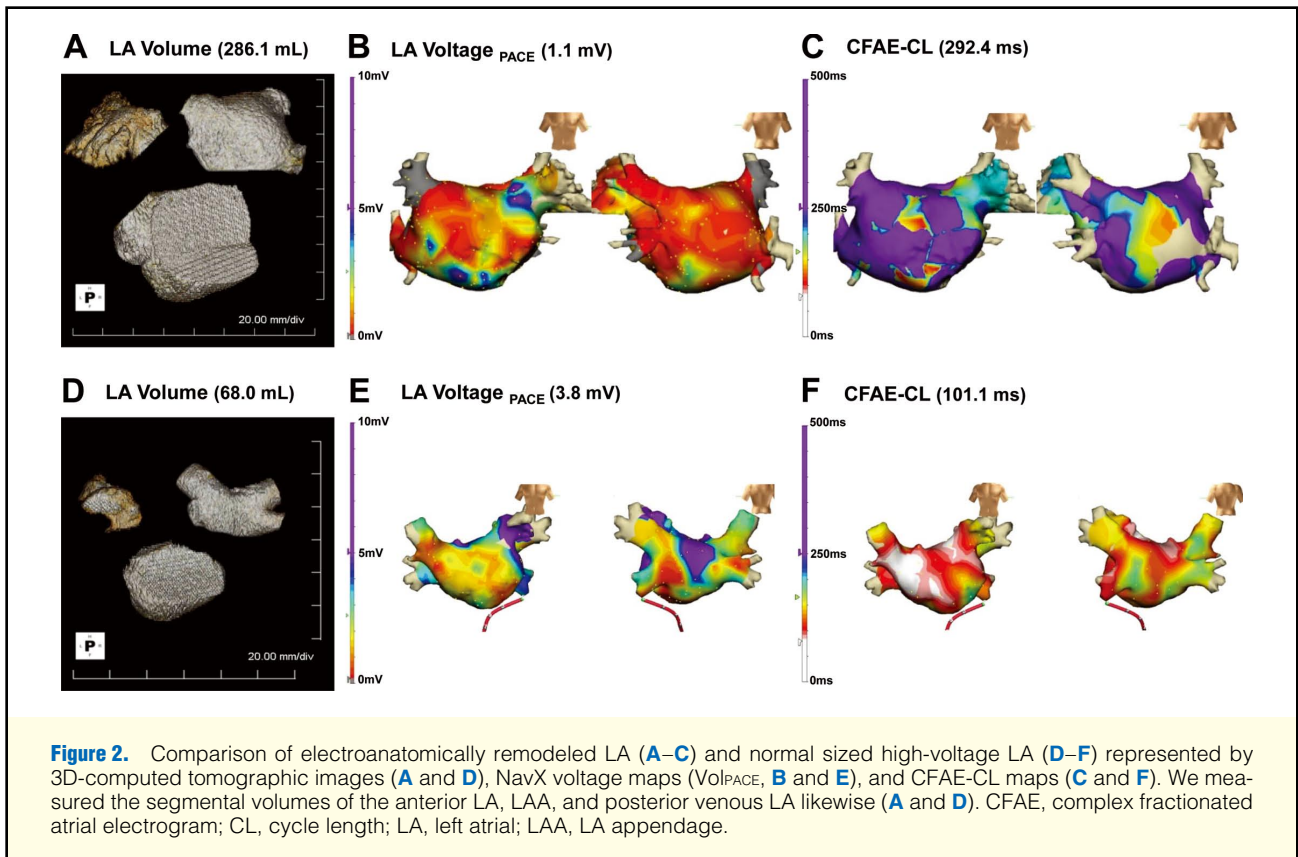
**Figure 1.** (A) Color-coded LA voltage map (Vol<sub>PACE</sub>) during high right atrial pacing 500ms. (B) Color-coded LA voltage map during AF (Vol<sub>AF</sub>). Vol<sub>AF</sub> was calculated by averaging each color corresponding to the voltage on the scale bar. (C) Automated calculation of Vol<sub>AF</sub> by 1 second recording of contact bipolar electrogram during AF. (D) Manual calculation of the average voltage during AF by measuring peak-to-peak voltages of AF electrograms within 1 second recording of the same segment used in panel (C). AF, atrial fibrillation; LA, left atrial.

were: (1) permanent AF refractory to electrical cardioversion; (2) LA >50mm measured on echocardiogram; (3) AF with rheumatic valvular disease; (4) associated structural heart disease other than left ventricular hypertrophy; (5) prior AF ablation; and (6) SR not maintained for LA voltage mapping before RFCA. Patients with LA thrombus were excluded by transesophageal echocardiography. We imaged all patients with 3D spiral CT (64 Channel, Light Speed Volume CT, Philips, Brilliance 63, the Netherlands) to visually define the anatomy of the LA and PVs.

### Electrophysiological Mapping Procedure

Intracardiac electrograms were recorded using the Prucka CardioLab™ Electrophysiology system (General Electric Medical Systems) and the catheter ablation procedure was performed on all patients using 3-D electroanatomical mapping (NavX, St Jude Medical) merged with 3-D spiral CT. Before performing catheter ablation, we generated a 3-D electroanatomical map of the LA, a CFAE-CL map, and a voltage map by obtaining contact bipolar electrograms filtered from 32 to 300Hz. If the initial rhythm was sustained AF, the CFAE-CL map was acquired first. To generate a CFAE-CL map, contact bipolar electrograms of AF were obtained for longer than 6s at each site approximately equally distributed

within the LA. The CFAE-CL was calculated by averaging the peak-to-peak intervals of 6-s recordings of bipolar electrograms.<sup>14,15</sup> The detection of the CFAE-CL also possessed a downstroke morphology in which the leading local-maximum and the trailing local-minimum amplitudes occurred within a time duration that was set to avoid detection of broad, far-field events, and to exceed a refractory period from the previous detection that was set to avoid multiple detections on a single deflection.<sup>14,15</sup> CFAE map settings were a refractory period of 49ms, P-P sensitivity >0.1mV, and duration of 30ms. After obtaining the CFAE-CL map, AF was terminated by internal cardioversion (2–10J, biphasic shocks with R wave synchronization, anodal decapolar catheter in the high right atrium to cathodal duo-decapolar catheter inside the coronary sinus; Lifepak12, Physiocontrol Ltd), and then a voltage map was generated. If the initial rhythm was SR, we acquired the LA voltage map first. Voltage maps were generated by recording bipolar electrograms and measuring peak-to-peak voltage (Vol<sub>PACE</sub>) during high right atrial pacing with a CL of 500ms. We did not obtain a LA voltage map if frequent reinitiation of AF required electrical cardioversion more than 3 times. As a result, LA voltage maps were obtained from 31 patients. The CFAE-CL maps and Vol<sub>PACE</sub> maps (Figure 1A) were color-coded, and the CFAE-CL maps were converted



into AF voltage ( $Vol_{AF}$ ) maps (**Figure 1B**) by software.  $Vol_{AF}$  was calculated by the maximal peak-to-peak voltage of the last 1-s bipolar electrogram recorded during the acquisition of the 6-s CFAE map (**Figures 1C,D**).

#### Off-Line Analyses of Color-Coded 3D Maps of LA

We analyzed 3 color-coded maps: CFAE-CL,  $Vol_{PACE}$ , and  $Vol_{AF}$ . Both anterior–posterior (AP) and posterior–anterior (PA) views of each map were captured and converted into image files. Each of the 6 color map images per patient (AP and PA views of the 3 color maps) were divided into 4 quadrants, and the percentages of the colored areas were measured and calculated.<sup>12</sup> The proportions of the color-coded areas in each quadrant (8 quadrants per patient) of the 3 different maps were analyzed by customized software (Image Pro), and were referenced to the color scale bars. We defined the CFAE area as white, and pink as an area with a CFAE-CL  $\leq 120$  ms.<sup>4</sup> The low-voltage area was defined as an area with an LA voltage  $< 0.2$  mV, and was color-coded gray; the high-voltage areas ( $> 5.0$  mV) were coded as purple, as described before.<sup>11</sup>

#### Volumetric and Curvilinear Lengths Analyses of 3D Spiral CT Imaging

The 3D spiral CT images of the LA were analyzed on an imaging processing workstation (Aquarius, Terarecon, USA) as described in our previous study.<sup>12</sup> The curvilinear lengths of the LA were measured at the linear ablation sites: bilateral antral ablation line, roof line, posterior inferior line, left lateral isthmus line, and anterior line. Each LA image was divided into portions by embryological origin as follows: the venous LA (posterior LA including the antrum and posterior wall), anterior LA (excluding the LAA and venous LA), and LAA.<sup>16</sup>

Although both the LAA and anterior LA are of embryological primordial atrial origin, they differ in geometry, myocardial fiber orientation, and the distribution of autonomic innervation. Therefore, we divided the LAA and anterior LA, and referenced them to points of inflection and separated the venous LA and anterior LA along the anterior border of both antral ablation lines, roof line, and posterior inferior line on the 3D spiral CT image (**Figures 2A,D**). The absolute and relative volumes of each portion were calculated and compared.

#### Data Analyses

We compared the mean and regional CFAE-CL with  $Vol_{PACE}$ ,  $Vol_{AF}$ , absolute or relative volumes of the embryological portions of the LA, and the length of the linear ablation lines on 3D spiral CT images. We also correlated  $Vol_{PACE}$  and  $Vol_{AF}$ . To validate  $Vol_{AF}$ , we compared the automatically measured  $Vol_{AF}$  and manually calculated mean voltage of AF electrogram within 1 s of the same segment acquired from 100 different sites. For statistical analyses, we decided the cut-offs as the median rounded to zero decimal places for LA volume and decimal 0.1 for LA voltage, and validated them by receiver-operating characteristic curve analyses. Data are expressed as the mean  $\pm$  standard deviation. Statistical significance of the comparisons was assessed using the Kruskal-Wallis test, and Student's t-test. A P-value  $< 0.05$  was considered significant.

## Results

### Low Voltage in Enlarged LA

**Figure 2** shows representative 3D-CT images of the LA, LA voltage maps, and CFAE maps. LA voltage was lower

|                                | LA volume<br>≥125 ml<br>(n=49) | LA volume<br><125 ml<br>(n=51) | P value |
|--------------------------------|--------------------------------|--------------------------------|---------|
| <b>CFAE-CL (ms)</b>            |                                |                                |         |
| Entire LA                      | 209.6±83.4                     | 165.7±73.0                     | 0.003   |
| Venous LA                      | 188.6±92.7                     | 150.8±80.9                     | 0.016   |
| LAA                            | 173.1±88.5                     | 138.9±70.8                     | 0.017   |
| Anterior LA                    | 206.1±86.2                     | 161.2±75.8                     | 0.003   |
| Left lateral isthmus area      | 243.2±108.5                    | 193.2±103.7                    | 0.010   |
| <b>% Area of CFAE</b>          |                                |                                |         |
| Entire LA                      | 28.4±26.8                      | 42.7±28.8                      | 0.006   |
| Venous LA                      | 20.6±27.2                      | 35.6±30.1                      | 0.005   |
| LAA                            | 39.3±34.3                      | 49.4±36.3                      | 0.077   |
| Anterior LA                    | 30.4±28.4                      | 45.7±30.9                      | 0.006   |
| Left lateral isthmus area      | 19.2±30.7                      | 34.4±35.2                      | 0.012   |
| <b>Vol<sub>PACE</sub> (mV)</b> |                                |                                |         |
| Entire LA                      | 1.4±0.7                        | 2.2±0.8                        | 0.005   |
| Venous LA                      | 1.4±1.0                        | 2.6±1.4                        | 0.004   |
| LAA                            | 2.5±1.7                        | 4.1±1.7                        | 0.008   |
| Anterior LA                    | 1.3±0.6                        | 1.7±0.6                        | 0.041   |
| Left lateral isthmus area      | 1.5±1.0                        | 1.9±0.9                        | 0.124   |
| <b>Vol<sub>AF</sub> (mV)</b>   |                                |                                |         |
| Entire LA                      | 0.6±0.3                        | 0.8±0.3                        | 0.003   |
| Venous LA                      | 0.6±0.4                        | 0.7±0.4                        | 0.017   |
| LAA                            | 1.3±1.1                        | 1.4±0.9                        | 0.247   |
| Anterior LA                    | 0.6±0.3                        | 0.7±0.2                        | 0.001   |
| Left lateral isthmus area      | 0.6±0.4                        | 0.9±0.7                        | 0.006   |

LA, left atrium; CFAE, complex fractionated atrial electrogram; CL, cycle length; LAA, left atrial appendage; Vol<sub>PACE</sub>, LA voltage map during high right atrial pacing; Vol<sub>AF</sub>, voltage map during atrial fibrillation.

(Figures 2A,B) in patients with an enlarged LA than in patients without LA enlargement (Figures 2D,E). Table 1 summarizes the patterns of LA voltage and CFAE in patients with 3D-CT measured LA volume ≥125 ml and <125 ml. The mean Vol<sub>PACE</sub> was significantly lower (1.4±0.7 mV vs 2.2±0.8 mV, P=0.005) in patients with LA ≥125 ml than those with <125 ml. Lower Vol<sub>PACE</sub> in an enlarged LA pattern was consistent in the different segments of venous LA, anterior LA, or LAA. Vol<sub>PACE</sub> and LA volume were negatively correlated (R=-0.5644, P<0.001; Figure 3A).

To validate the automatically measured Vol<sub>AF</sub>, we calculated the mean values of manually measured peak-to-peak voltages from 1-s AF electrograms in 100 different segments, and compared them with the automatically measured Vol<sub>AF</sub> in the same segments by a single investigator who was blinded to all the data (Figures 1C,D). The automatically measured maximal peak-to-peak Vol<sub>AF</sub> showed good correlation with the manually calculated mean voltage during AF (R=0.8224, P<0.0001; Figure 3B). We also compared the mean LA Vol<sub>AF</sub> with the mean Vol<sub>PACE</sub> of the same patient, and found a correlation between them (R=0.6155, P<0.0001; Figure 3C).

### Prolonged CFAE-CL and Shrinking CFAE Area in Electroanatomically Remodeled LA

In patients with an electroanatomically remodeled LA (ie, enlarged LA with low mean LA voltage) the CFAE-CL was low and % area of CFAE smaller (Figures 2A-C) than in those without a remodeled LA (Figures 2D-F). When we

|                                    | Vol <sub>PACE</sub><br><1.7 mV | Vol <sub>PACE</sub><br>≥1.7 mV | P value |
|------------------------------------|--------------------------------|--------------------------------|---------|
| <b>LA volume (ml)</b>              |                                |                                |         |
| Entire LA                          | 155.7±58.0                     | 92.6±34.7                      | <0.001  |
| Venous LA                          | 47.5±21.4                      | 33.7±12.4                      | 0.016   |
| LAA                                | 15.3±7.9                       | 7.8±3.2                        | 0.001   |
| Anterior LA                        | 92.8±38.1                      | 51.0±21.0                      | <0.001  |
| Right antral volume                | 11.6±4.3                       | 8.7±2.9                        | 0.018   |
| Left antral volume                 | 11.0±5.5                       | 9.5±4.0                        | 0.194   |
| <b>Proportional LA volumes (%)</b> |                                |                                |         |
| Venous LA                          | 30.6±8.2                       | 36.9±5.0                       | 0.006   |
| LAA                                | 10.2±4.2                       | 8.7±2.5                        | 0.114   |
| Anterior LA                        | 59.3±9.1                       | 54.4±5.9                       | 0.043   |
| Right antral volume                | 7.6±1.7                        | 9.9±2.9                        | 0.006   |
| Left antral volume                 | 7.6±3.8                        | 10.5±3.6                       | 0.020   |
| <b>CFAE-CL (ms)</b>                |                                |                                |         |
| Entire LA                          | 203.4±78.3                     | 128.3±55.9                     | 0.002   |
| Venous LA                          | 221.3±82.2                     | 134.0±62.6                     | 0.001   |
| LAA                                | 164.0±74.5                     | 103.1±57.3                     | 0.008   |
| Anterior LA                        | 199.8±88.8                     | 126.1±57.9                     | 0.005   |
| Left lateral isthmus area          | 201.2±95.7                     | 155.2±88.8                     | 0.088   |
| <b>% Area of CFAE</b>              |                                |                                |         |
| Entire LA                          | 30.8±26.2                      | 58.0±30.0                      | 0.006   |
| Venous LA                          | 18.4±23.5                      | 52.9±32.3                      | 0.001   |
| LAA                                | 42.6±31.7                      | 67.4±32.6                      | 0.021   |
| Anterior LA                        | 34.9±30.6                      | 60.4±31.3                      | 0.015   |
| Left lateral isthmus area          | 28.5±38.0                      | 45.1±37.3                      | 0.115   |

Abbreviations see in Table 1.

compared the patients with LA volume ≥125 ml and those with <125 ml, both the mean CFAE-CL and the regional CFAE-CL were lower in patients with an enlarged LA (Table 1). The % area of CFAE was also lower in patients with LA ≥125 ml than in those with <125 ml. LA volume showed a weak positive correlation with CFAE-CL (R=0.4509, P<0.0001) and weak negative correlation with % area of CFAE (R=-0.3902, P<0.0001).

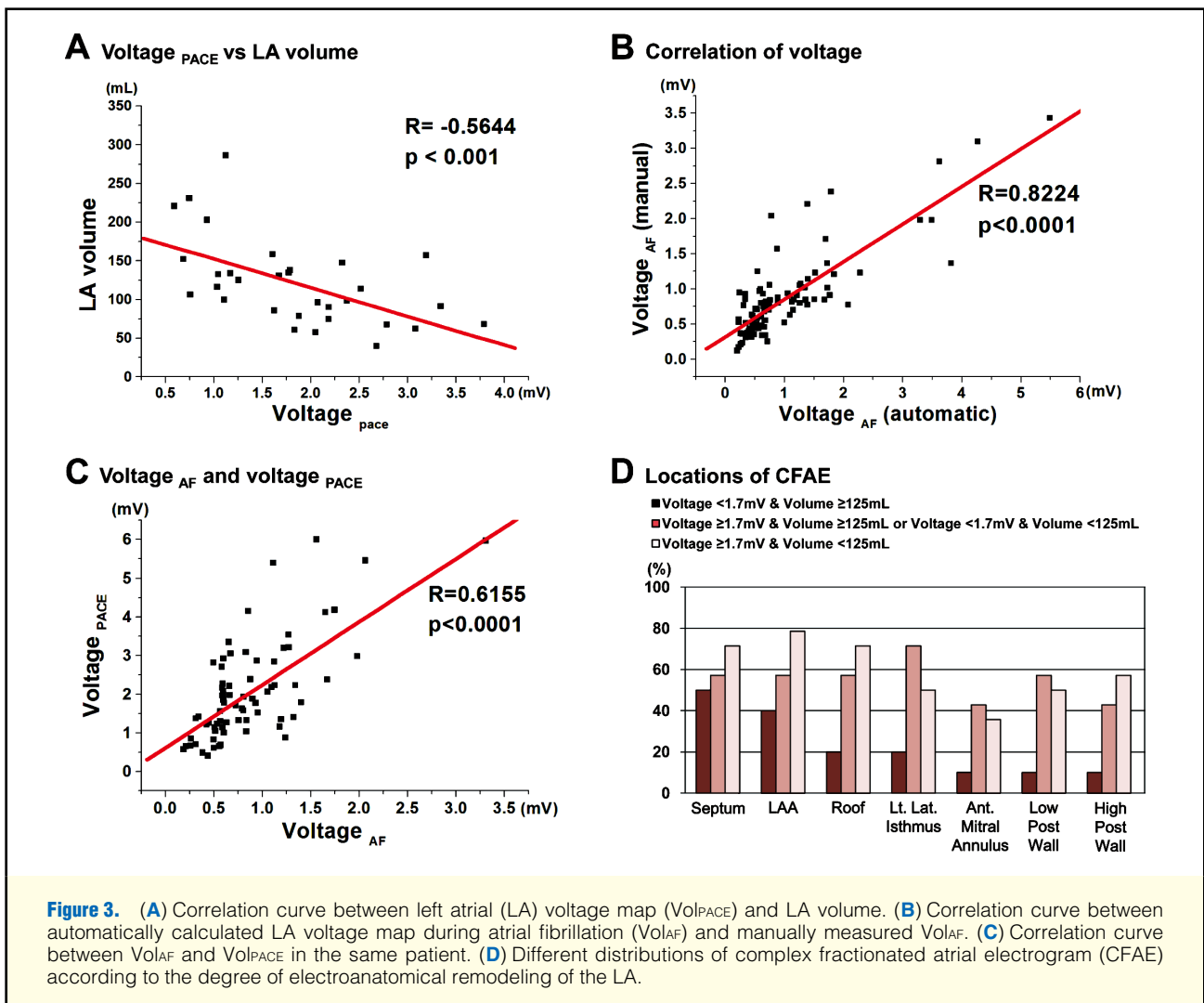
When we compared the patients with mean LA Vol<sub>PACE</sub> <1.7 mV with those with ≥1.7 mV (Table 2), or mean LA Vol<sub>AF</sub> ≤0.7 mV with those with >0.7 mV, the mean CFAE-CL and the regional CFAE-CL were longer (P=0.002) and the % area of CFAE was lower (P=0.006) in patients with a low-voltage LA. Entire LA volume and regional LA volume were greater in patients with a low-LA voltage, which is consistent with the data shown in Table 1.

### Distribution of CFAE in Electroanatomically Remodeled LA

Figure 3D shows the distribution of CFAE according to the degree of electroanatomical remodeling. We compared patients with LA Vol<sub>PACE</sub> ≤1.7 mV and LA volume ≥125 ml, those with LA Vol<sub>PACE</sub> ≥1.7 mV and LA volume <125 ml, and those with an intermediate degree of remodeling. The incidence of septal CFAE was consistently high, regardless of the degree of LA remodeling, and the incidence of CFAE in other areas was reduced in the electroanatomically remodeled LA compared with a less remodeled LA.

## Discussion

In this study, we have documented different patterns of CFAE



in patients with an electroanatomically remodeled LA. CFAE-CL was longer and the % area of CFAE was lower in patients with an enlarged LA or low-voltage LA. Although the actual location of the CFAE differed among patients with a remodeled atrium, it was consistently positioned on the septum. These findings suggest that the patterns of CFAE are closely related to the degree of electroanatomical remodeling of the LA. We also documented a moderate correlation between  $Vol_{PACE}$  and  $Vol_{AF}$ .

### CFAE in AF Ablation

Although the mechanism of CFAE has not yet been clearly elucidated, electrogram-guided RFCA targeting CFAE has been used as a substrate modification strategy in the catheter ablation of AF, especially for patients with PeAF. CFAE was first mentioned by Konings et al as an intraoperative mapping of human AF.<sup>17</sup> Nademanee et al reported excellent clinical outcomes of CFAE-guided LA ablation.<sup>4,5</sup> It has been demonstrated that 66–95% of cases of sustained AFs were terminated or organized during CFAE-guided AF ablation,<sup>4,8–10,18</sup> which strongly indicates that the CFAE locus plays an important role in the maintenance of AF. In contrast, the clinical outcomes of CFAE ablation in other reports have varied widely, with SR maintenance rates ranging between 54% and

74%.<sup>6,8,10</sup> CFAE-guided AF ablation has the limitation of differentiating CFAE with active driver and passive wave-breaker. Takahashi et al reported that only 17% of the CFAE areas were related to the termination of AF.<sup>9</sup> Therefore, CFAE can be affected by temporal phenomenon caused by autonomic activity<sup>19–21</sup> or electrical remodeling.<sup>22</sup> In this study, the CFAE-CL was shorter and % area of CFAE was larger in patients with a normal-sized, high-voltage LA as compared with the electroanatomically remodeled atrium. The distribution of CFAE was also different. Most cases of PAF with a normal-sized LA without electrical remodeling have an excellent clinical outcome after circumferential PV isolation without additional CFAE-electrogram-guided AF ablation.<sup>23</sup> Therefore, CFAE alone may not be a parameter sufficient to explain the pathophysiology of AF, at least in patients without electroanatomical remodeling of the LA.

### CFAE in the Remodeled LA

Long-lasting AF induces atrial dilatation by changing LA function, increasing interstitial fibrosis, and atriomypathy.<sup>24,25</sup> LA pressure contributes to AF initiation and maintenance,<sup>26</sup> and LA ischemia reduces conduction velocity, which makes it susceptible to reentry maintenance.<sup>27</sup> Atrial structural remodeling accompanies ultrastructural changes<sup>28–30</sup> (ie, electrical

remodeling), such as downregulation of the L-type calcium channel ( $I_{Ca-L}$ ) and delayed rectification of the potassium channel ( $I_{Kr}$ ), leading to reduced conduction velocity.<sup>26</sup> Neurohormonal activations, such as atrial natriuretic peptide, brain natriuretic peptide or the renin–angiotensin–aldosterone axis, result in inflammation and fibrosis.<sup>31</sup> The AF-related reduction in endocardial voltage is associated with local conduction slowdown, which plays a major role in promoting AF.<sup>28,32</sup> In the present study, the CFAE-CL was longer and % area of CFAE lower in patients with an electroanatomically remodeled LA than in those without it. In contrast, Sanders et al reported higher dominant frequency (DF) in the atria of patients with PeAF and electroanatomical remodeling compared with PAF patients.<sup>33</sup> These results seem to contradict each other. However, the site of the CFAE does not match exactly the location of the DF,<sup>15</sup> and the actual site exists at the boundaries of the maximal DF domain.<sup>34</sup> Although both DF and CFAE reflect the frequency of the local electrogram, refractoriness, conduction velocity, and tissue anisotropy at the location of the electrogram, the former is a simple mathematical number of the fibrillation waveform (Fast Fourier transformation) and the latter is affected by the morphology and amplitude of the electrogram. Differences in recording systems or filter settings may also contribute to this difference. Therefore, we found that CFAE-CL was reduced in patients with AF and an electroanatomically remodeled LA with lowered conduction velocity, in contrast to DF.

### Study Limitations

The patients included in this study were a highly selective group referred for RFCA. Although we detected CFAE with an adaptive peak-to-peak sensitivity threshold  $>0.1$  mV, some CFAEs with low voltage might be considered as low voltage noise in patients with PeAF. We detected CFAE using a specific algorithm in the time domain, primarily based on the CL, so the findings of this study may not be directly comparable with other studies that used different parameters to identify CFAE. Because we acquired CFAE-CLs by point-by-point contact mapping, the CFAE-CL maps did not reflect a spatiotemporally homogeneous distribution of CFAE. We analyzed 3D maps using 2D measurements.

### Conclusion

We documented different patterns of CFAE in patients with an electroanatomically remodeled LA. CFAE-CL was longer and % area of CFAE was lower in patients with an enlarged LA or low-voltage LA. The actual location of the CFAE differed among patients with a remodeled atrium, but it was consistently positioned on the septum. These findings suggest that pattern of CFAE is closely related to the degree of electroanatomical remodeling of the LA.

### Acknowledgments

This work was supported by a grant of the Korea Health 21 R&D Project (A085136), Ministry of Health & Welfare, Republic of Korea, and the Korean Society of Circulation Industry-University Cooperation.

### Disclosure

No conflicts to disclose.

### References

1. Oral H, Pappone C, Chugh A, Good E, Bogun F, Pelosi F Jr, et al. Circumferential pulmonary-vein ablation for chronic atrial fibrillation. *N Engl J Med* 2006; **354**: 934–941.
2. Pappone C, Santinelli V, Manguso F, Vicedomini G, Gugliotta F, Augello G, et al. Pulmonary vein denervation enhances long-term benefit after circumferential ablation for paroxysmal atrial fibrillation. *Circulation* 2004; **109**: 327–334.
3. Oral H, Knight BP, Tada H, Ozaydin M, Chugh A, Hassan S, et al. Pulmonary vein isolation for paroxysmal and persistent atrial fibrillation. *Circulation* 2002; **105**: 1077–1081.
4. Nademanee K, McKenzie J, Kosar E, Schwab M, Sunsaneewitayakul B, Vasavakul T, et al. A new approach for catheter ablation of atrial fibrillation: Mapping of the electrophysiologic substrate. *J Am Coll Cardiol* 2004; **43**: 2044–2053.
5. Nademanee K, Schwab MC, Kosar EM, Karwecki M, Moran MD, Visessook N, et al. Clinical outcomes of catheter substrate ablation for high-risk patients with atrial fibrillation. *J Am Coll Cardiol* 2008; **51**: 843–849.
6. Oral H, Chugh A, Good E, Wimmer A, Dey S, Gadeela N, et al. Radiofrequency catheter ablation of chronic atrial fibrillation guided by complex electrograms. *Circulation* 2007; **115**: 2606–2612.
7. Verma A, Patel D, Famy T, Martin DO, Burkhardt JD, Elayi SC, et al. Efficacy of adjuvant anterior left atrial ablation during intracardiac echocardiography-guided pulmonary vein antrum isolation for atrial fibrillation. *J Cardiovasc Electrophysiol* 2007; **18**: 151–156.
8. Estner HL, Hessling G, Ndrepepa G, Luik A, Schmitt C, Konietzko A, et al. Acute effects and long-term outcome of pulmonary vein isolation in combination with electrogram-guided substrate ablation for persistent atrial fibrillation. *Am J Cardiol* 2008; **101**: 332–337.
9. Takahashi Y, O'Neill MD, Hocini M, Dubois R, Matsuo S, Knecht S, et al. Characterization of electrograms associated with termination of chronic atrial fibrillation by catheter ablation. *J Am Coll Cardiol* 2008; **51**: 1003–1010.
10. Schmitt C, Estner H, Hecher B, Luik A, Kolb C, Karch M, et al. Radiofrequency ablation of complex fractionated atrial electrograms (CFAE): Preferential sites of acute termination and regularization in paroxysmal and persistent atrial fibrillation. *J Cardiovasc Electrophysiol* 2007; **18**: 1039–1046.
11. Park JH, Pak HN, Kim SK, Jang JK, Choi JI, Lim HE, et al. Electrophysiologic characteristics of complex fractionated atrial electrograms in patients with atrial fibrillation. *J Cardiovasc Electrophysiol* 2009; **20**: 266–272.
12. Park JH, Pak HN, Choi EJ, Jang JK, Kim SK, Choi DH, et al. The Relationship between endocardial voltage and regional volume in electroanatomically remodeled left atria in patients with atrial fibrillation: Comparison of three-dimensional computed tomographic images and voltage mapping. *J Cardiovasc Electrophysiol* 2009; **20**: 1349–1356.
13. Stiles MK, John B, Wong CX, Kuklik P, Brooks AG, Lau DH, et al. Paroxysmal lone atrial fibrillation is associated with an abnormal atrial substrate: Characterizing the “second factor”. *J Am Coll Cardiol* 2009; **53**: 1182–1191.
14. Lin YJ, Tai CT, Kao T, Chang SL, Wongcharoen W, Lo LW, et al. Consistency of complex fractionated atrial electrograms during atrial fibrillation. *Heart Rhythm* 2008; **5**: 406–412.
15. Stiles MK, Brooks AG, John B, Wilson L, Kuklik P, Dimitri H, et al. The effect of electrogram duration on quantification of complex fractionated atrial electrograms and dominant frequency. *J Cardiovasc Electrophysiol* 2008; **19**: 252–258.
16. Douglas YL, Jongbloed MR, Gittenberger-de Groot AC, Evers D, Dion RA, Voigt P, et al. Histology of vascular myocardial wall of left atrial body after pulmonary venous incorporation. *Am J Cardiol* 2006; **97**: 662–670.
17. Konings KT, Smeets JL, Penn OC, Wellens HJ, Allessie MA. Configuration of unipolar atrial electrograms during electrically induced atrial fibrillation in humans. *Circulation* 1997; **95**: 1231–1241.
18. Porter M, Spear W, Akar JG, Helms R, Brysiewicz N, Santucci P, et al. Prospective study of atrial fibrillation termination during ablation guided by automated detection of fractionated electrograms. *J Cardiovasc Electrophysiol* 2008; **19**: 613–620.
19. Lin J, Scherlag BJ, Zhou J, Lu Z, Patterson E, Jackman WM, et al. Autonomic mechanism to explain complex fractionated atrial electrograms (CFAE). *J Cardiovasc Electrophysiol* 2007; **18**: 1197–1205.
20. Lemery R, Birnie D, Tang AS, Green M, Gollob M. Feasibility study of endocardial mapping of ganglionated plexuses during catheter ablation of atrial fibrillation. *Heart Rhythm* 2006; **3**: 387–396.
21. Furukawa T, Hirao K, Horikawa-Tanami T, Hachiya H, Isobe M. Influence of autonomic stimulation on the genesis of atrial fibrillation in remodeled canine atria not the same as in normal atria. *Circ J* 2009; **73**: 468–475.
22. Goette A, Honeycutt C, Langberg JJ. Electrical remodeling in atrial fibrillation: Time course and mechanisms. *Circulation* 1996; **94**:

- 2968–2974.
23. Pak HN, Kim JS, Shin SY, Lee HS, Choi JI, Lim HE, et al. Is empirical four pulmonary vein isolation necessary for focally triggered paroxysmal atrial fibrillation? Comparison of selective pulmonary vein isolation versus empirical four pulmonary vein isolation. *J Cardiovasc Electrophysiol* 2008; **19**: 473–479.
  24. Hoit BD, Shao Y, Gabel M, Walsh RA. Left atrial mechanical and biochemical adaptation to pacing induced heart failure. *Cardiovasc Res* 1995; **29**: 469–474.
  25. Choi JI, Park SM, Park JS, Hong SJ, Pak HN, Lim do S, et al. Changes in left atrial structure and function after catheter ablation and electrical cardioversion for atrial fibrillation. *Circ J* 2008; **72**: 2051–2057.
  26. Li D, Melnyk P, Feng J, Wang Z, Petrecca K, Shrier A, et al. Effects of experimental heart failure on atrial cellular and ionic electrophysiology. *Circulation* 2000; **101**: 2631–2638.
  27. Sinno H, Derakhchan K, Libersan D, Merhi Y, Leung TK, Nattel S. Atrial ischemia promotes atrial fibrillation in dogs. *Circulation* 2003; **107**: 1930–1936.
  28. Li D, Fareh S, Leung TK, Nattel S. Promotion of atrial fibrillation by heart failure in dogs: Atrial remodeling of a different sort. *Circulation* 1999; **100**: 87–95.
  29. Boixel C, Fontaine V, Rucker-Martin C, Milliez P, Louedec L, Michel JB, et al. Fibrosis of the left atria during progression of heart failure is associated with increased matrix metalloproteinases in the rat. *J Am Coll Cardiol* 2003; **42**: 336–344.
  30. Ausma J, Wijffels M, Thone F, Wouters L, Allessie M, Borgers M. Structural changes of atrial myocardium due to sustained atrial fibrillation in the goat. *Circulation* 1997; **96**: 3157–3163.
  31. Casacang-Verzosa G, Gersh BJ, Tsang TS. Structural and functional remodeling of the left atrium: Clinical and therapeutic implications for atrial fibrillation. *J Am Coll Cardiol* 2008; **51**: 1–11.
  32. Appleton CP, Galloway JM, Gonzalez MS, Gaballa M, Basnight MA. Estimation of left ventricular filling pressures using two-dimensional and Doppler echocardiography in adult patients with cardiac disease: Additional value of analyzing left atrial size, left atrial ejection fraction and the difference in duration of pulmonary venous and mitral flow velocity at atrial contraction. *J Am Coll Cardiol* 1993; **22**: 1972–1982.
  33. Sanders P, Berenfeld O, Hocini M, Jais P, Vaidyanathan R, Hsu LF, et al. Spectral analysis identifies sites of high-frequency activity maintaining atrial fibrillation in humans. *Circulation* 2005; **112**: 789–797.
  34. Kalifa J, Tanaka K, Zaitsev AV, Warren M, Vaidyanathan R, Auerbach D, et al. Mechanisms of wave fractionation at boundaries of high-frequency excitation in the posterior left atrium of the isolated sheep heart during atrial fibrillation. *Circulation* 2006; **113**: 626–633.